Inorganic Chemistry
Article

*Inorg. Chem.* **2010**, *49*, 11637–11642 **11637**
DOI: 10.1021/ic101935f

# Functional Mesoporous Metal−Organic Frameworks for the Capture of Heavy Metal Ions and Size-Selective Catalysis

**Qian-Rong Fang, Da-Qian Yuan, Julian Sculley, Jian-Rong Li, Zheng-Bo Han, and Hong-Cai Zhou***

*Department of Chemistry, Texas A&M University, College Station, Texas 77842, United States*

Received September 21, 2010

By using $Zn_4O(CO_2)_6$ as secondary building units (SBUs) and two extended ligands containing amino functional groups, TATAB and BTATB (TATAB = 4,4′,4″-s-triazine-1,3,5-triyltri-*p*-aminobenzoate and BTATB = 4,4′,4″-(benzene-1,3,5-triyltris(azanediyl))tribenzoate), two isostructural mesoporous metal−organic frameworks (MOFs) with cavities up to 2.73 nm, designated as PCN-100 and PCN-101 (PCN represents porous coordination network), have been synthesized. $N_2$ sorption isotherms of both PCN-100 and -101 showed typical type IV behavior, indicating their mesoporous nature. The TATAB ligand that comprises PCN-100 was employed to capture heavy metal ions (Cd(II) and Hg(II)) by constructing complexes within the pores with a possible coordination mode similar to that found in aminopyridinato complexes. This reveals that mesoporous materials such as PCN-100 can be applied in the elimination of heavy metal ions from waste liquid. In addition, both PCNs-100 and -101 exhibit size-selective catalytic activity toward the Knoevenagel condensation reaction.

## 1. Introduction

Over the past decade, porous metal−organic frameworks (MOFs) have attracted much attention due to their unique structures and numerous potential applications as functional materials.[1−19] One limiting factor in MOFs catching on as a primary source for porous materials is the unfortunate scarcity of mesoporous MOFs. So far, the majority of all reported porous MOFs are microporous (with pore sizes less than 2 nm). Only a few mesoporous MOFs, containing channel or cavity sizes in the plus 2 nm realm, have recently been reported. These MOFs brimmed with application potential in gas storage, separation, sensor, catalysis, and drug delivery.[20−29] For instance, Yaghi et al. prepared a 3-D mesoporous MOF with channels sizes of 28.8 Å, designated as IRMOF-16, by using a linear linker, TPDC (TPDC = [1,1′:4′,1″-terphenyl]-4,4″-dicarboxylate) and $Zn_4O(CO_2)_6$ secondary building unit

*To whom correspondence should be addressed. E-mail: zhou@mail.chem.tamu.edu.

(1) Furukawa, H.; Ko, N.; Go, Y. B.; Aratani, N.; Choi, S. B.; Choi, E.; Yazaydin, A. O.; Snurr, R. Q.; O'Keeffe, M.; Kim, J.; Yaghi, O. M. *Science* **2010**, *329*, 424–428.
(2) Shimomura, S.; Higuchi, M.; Matsuda, R.; Yoneda, K.; Hijikata, Y.; Kubota, Y.; Mita, Y.; Kim, J.; Takata, M.; Kitagawa, S. *Nat. Chem.* **2010**, *2*, 633–637.
(3) Blake, A. J.; Champness, N. R.; Easun, T. L.; Allan, D. R.; Nowell, H.; George, M. W.; Jia, J.; Sun, X. Z. *Nat. Chem.* **2010**, *2*, 688–694.
(4) Férey, G.; Serre, C. *Chem. Soc. Rev.* **2009**, *38*, 1380–1399.
(5) Perry, J. J.; Perman, J. A.; Zaworotko, M. J. *Chem. Soc. Rev.* **2009**, *38*, 1400–1417.
(6) Wang, Z. Q.; Cohen, S. M. *Chem. Soc. Rev.* **2009**, *38*, 1315–1329.
(7) Ma, L. Q.; Abney, C.; Lin, W. B. *Chem. Soc. Rev.* **2009**, *38*, 1248–1256.
(8) Chui, S. S. Y.; Lo, S. M. F.; Charmant, J. P. H.; Orpen, A. G.; Williams, I. D. *Science* **1999**, *283*, 1148–1150.
(9) Li, H.; Eddaoudi, M.; O'Keeffe, M.; Yaghi, O. M. *Nature* **1999**, *402*, 276–279.
(10) James, S. L. *Chem. Soc. Rev.* **2003**, *32*, 276–288.
(11) Janiak, C. *Dalton Trans.* **2003**, 2781–2804.
(12) Rosseinsky, M. J. *Microporous Mesoporous Mater.* **2004**, *73*, 15–30.
(13) Seo, J. S.; Whang, D.; Lee, H.; Jun, S. I.; Oh, J.; Jeon, Y. J.; Kim, K. *Nature* **2000**, *404*, 982–986.
(14) Chen, B. L.; Eddaoudi, M.; Hyde, S. T.; O'Keeffe, M.; Yaghi, O. M. *Science* **2001**, *291*, 1021–1023.
(15) Fang, Q. R.; Zhu, G. S.; Xue, M.; Sun, J. Y.; Wei, Y.; Qiu, S. L.; Xu, R. R. *Angew. Chem., Int. Ed.* **2005**, *44*, 3845–3848.
(16) Pan, L.; Parker, B.; Huang, X. Y.; Olson, D. H.; Lee, J.; Li, J. *J. Am. Chem. Soc.* **2006**, *128*, 4180–4181.
(17) Ma, S. Q.; Zhou, H. C. *J. Am. Chem. Soc.* **2006**, *128*, 11734–11735.
(18) Dincă, M.; Long, J. R. *Angew. Chem., Int. Ed.* **2008**, *47*, 6766–6779.
(19) Zhang, J.; Chen, S. M.; Wu, T.; Feng, P. Y.; Bu, X. H. *J. Am. Chem. Soc.* **2008**, *130*, 12882–12883.
(20) Eddaoudi, M.; Kim, J.; Rosi, N.; Vodak, D.; Wachter, J.; O'Keeffe, M.; Yaghi, O. M. *Science* **2002**, *295*, 469–472.
(21) Férey, G.; Serre, C.; Mellot-Draznieks, C.; Millange, F.; Surblé, S.; Dutour, J.; Margiolaki, I. *Angew. Chem., Int. Ed.* **2004**, *43*, 6296–6301.
(22) Férey, G.; Mellot-Draznieks, C.; Serre, C.; Millange, F.; Dutour, J.; Surblé, S.; Margiolaki, I. *Science* **2005**, *309*, 2040–2042.
(23) Wang, X. S.; Ma, S. Q.; Sun, D. F.; Parkin, S.; Zhou, H. C. *J. Am. Chem. Soc.* **2006**, *128*, 16474–16475.
(24) Fang, Q. R.; Zhu, G. S.; Jin, Z.; Ji, Y. Y.; Ye, J. W.; Xue, M.; Yang, H.; Wang, Y.; Qiu, S. L. *Angew. Chem., Int. Ed.* **2007**, *46*, 6638–6642.
(25) Park, Y. K.; Choi, S. B.; Kim, H.; Kim, K.; Won, B. H.; Choi, K.; Choi, J. S.; Ahn, W. S.; Won, N.; Kim, S.; Jung, D. H.; Choi, S. H.; Kim, G. H.; Cha, S. S.; Jhon, Y. H.; Yang, J. K.; Kim, J. *Angew. Chem., Int. Ed.* **2007**, *46*, 8230–8233.
(26) Wang, B.; Cote, A. P.; Furukawa, H.; O'Keeffe, M.; Yaghi, O. M. *Nature* **2008**, *453*, 207–211.
(27) Koh, K.; Wong-Foy, A. G.; Matzger, A. J. *Angew. Chem., Int. Ed.* **2008**, *47*, 677–680.
(28) Koh, K.; Wong-Foy, A. G.; Matzger, A. J. *J. Am. Chem. Soc.* **2009**, *131*, 4184–4185.
(29) Sonnauer, A.; Hoffmann, F.; Froba, M.; Kienle, L.; Duppel, V.; Thommes, M.; Serre, C.; Férey, G.; Stock, N. *Angew. Chem., Int. Ed.* **2009**, *48*, 3791–3794.


Published on Web 11/17/2010

(SBU).[20] However, no further characterization of $N_2$-sorption was reported, presumably due to the structural instability of the MOF after removal of guest molecules. Subsequently, we reported a noninterpenetrated mesoporous MOF, meso-MOF-1, with open channels of 22.5 × 26.1 Å$^2$ from all three orthogonal directions.[23] Most notably, $N_2$-sorption measurements of the MOF revealed a typical type IV isotherm, indicating the mesoporous nature of this material.

The augmentation of the sizes of channels or cavities of MOFs to the mesoporous range (2−50 nm) still poses a great challenge. Ligand extension is a favorable strategy; however, open MOFs constructed from large ligands tend to disintegrate after the removal of guest molecules. Another difficulty to obtaining mesoporous MOFs containing elongated ligands is how to inhibit framework interpenetration. Interpenetration occurs because it adds stability by drastically reducing the sizes of channels or cavities. The major drawback of interpenetration is clearly the obstruction of large molecules entering the internal pores thus limiting the application potential of the resulting MOFs. Therefore, the strategy for the preparation of mesoporous MOFs should focus on ligand extension, while preventing interpenetration, yet maximizing framework stability.

With the above considerations in mind, our strategy is to use $Zn_4O(CO_2)_6$ and extended trigonal planar ligands containing amino functional groups as SBUs to construct MOFs containing mesopores, while preventing interpenetration by ligand design and stabilizing the open framework through hydrogen bonding. Two such ligands, TATAB (TATAB = 4,4′,4″-s-triazine-1,3,5-triyltri-*p*-aminobenzoate) and BTATB (BTATB = 4,4′,4″-(benzene-1,3,5-triyltris(azanediyl))tribenzoate), were selected to construct mesoporous MOFs. The two ligands are more elongated than other trigonal planar ligands such as BTC,[2] BTB[30] and TATB[15] (Scheme 1). Another consideration in the design of these ligands was to include functional groups to increase the versatility of the resulting MOFs. Both ligands possess amino groups that are not involved in coordination bonds that make up the frameworks. The functional groups are left inside the framework as potential sites for size-selective catalysis or coordination with additional metal ions through postsynthetic treatment. Herein, we present two isostructural mesoporous MOFs, $Zn_4O(TATAB)_2\cdot 17(DEF)\cdot 3(H_2O)$ and $Zn_4O(BTATB)_2\cdot 16(DEF)\cdot 5(H_2O)$ (designated as PCN-100 and PCN-101, respectively; PCN = porous coordination network; DEF = *N*,*N*-diethylformamide), with cavities up to 2.73 nm. The $N_2$ sorption isotherms of both exhibit type IV behavior, typical of mesoporous materials. These mesoporous MOFs were exploited in two ways: PCN-100 was used to capture heavy metal ions, Cd(II) and Hg(II); both PCN-100 and PCN-101 were tested as catalysts for size-selective Knoevenagel condensation reactions.

## 2. Experimental Section

**General Information.** Commercially available reagents were used as received without further purification. Elemental analyses (C, H, and N) were obtained by Atlantic Microlab, Inc. Inductively coupled plasma (ICP) analyses were carried out on a Perkin-Elmer Optima 3300 DV ICP spectrometer. Nuclear magnetic resonance (NMR) data were collected on a Mercury 300 spectrometer. Powder X-ray diffraction patterns (PXRD) were recorded on a Bruker D8 Discover diffractometer equipped with a Cu sealed tube ($\lambda$ = 1.54178 Å) at a scan rate of 1 deg·s$^{-1}$. Powder samples were dispersed on low-background quartz discs (G. M. Associates, Inc., Oakland, California) for analyses. Simulation of the PXRD spectra was carried out by using the single-crystal data and diffraction-crystal module of the Mercury program available free of charge via Internet at http://www.ccdc.cam.ac.uk/products/mercury/. FT-IR data were recorded on an IRAffinity-1 instrument. Thermogravimetric analysis (TGA) was performed under a $N_2$ atmosphere on a TGA-50 (SHIMADZU) thermogravimetric analyzer with a heating rate of 2 °C min$^{-1}$.

**Scheme 1.** Some Examples of Planar Tricarboxylate Ligands

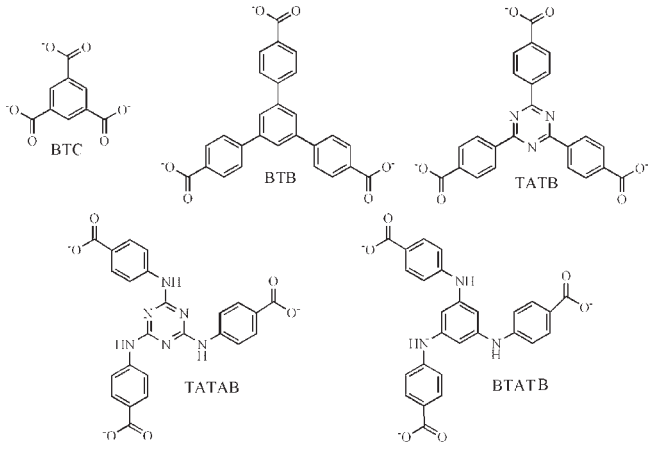


**Synthesis of $H_3$TATAB, 4,4′,4″-s-Triazine-1,3,5-triyltri-*p*-aminobenzoic Acid.** A solution of 4-aminobenzoic acid (1.8 g, 13.2 mmol) in 20.0 mL of water and 3.0 mL of 5 N sodium hydroxide was charged with sodium bicarbonate (0.9 g, 11.0 mmol). To this, a solution of cyanuric chloride (0.6 g, 3.3 mmol) in 5.0 mL of 1,4-dioxane, was slowly added. The mixture was stirred at room temperature for 10 min, then overnight at 110 °C. After cooling to room temperature, the solution was acidified with 20% hydrochloric acid to pH = 3. The suspension was centrifuged and the solid was washed with water. The light yellow powder was collected and dried in an oven to yield pure **$H_3$TATAB** (1.8 g, 80%). $^1$H NMR (DMSO-$d_6$): $\delta$ 7.87 (d, 6H), 7.97 (d, 6H), 9.84 (s, 3H), 12.55 (s, br, 3H).

**Synthesis of Triethyl 4,4′,4″-(Benzene-1,3,5-triyltris(azanediyl))-tribenzoate, 1.** Concentrated hydrochloric acid (5.2 mL), phloroglucinol (12.6 g, 10.0 mmol), 4-aminobenzoic acid ethyl ester (66.0 g, 40.0 mmol), and diethyleneglycol dimethylether (45 mL) were added to a 100 mL round-bottom flask, and stirred at 130 °C for 7 h. Yellow crystals appeared as the suspension was cooled. The crystals were washed with diethyleneglycol dimethylether and dried in an oven to yield **1** (35.2 g, 70%). $^1$H NMR (DMSO-$d_6$): $\delta$ 1.30 (t, 9H), 4.26 (q, 6H), 6.62 (s, 3H), 7.13 (d, 6H), 8.38 (d, 6H), 8.78 (s, 3H).

**Synthesis of $H_3$BTATB, 4,4′,4″-(Benzene-1,3,5-triyltris(azanediyl))tribenzoic Acid, 2.** Compound **1** (10.0 g, 19.0 mmol) was suspended in 150.0 mL THF/MeOH (v: v = 1: 1). A solution of 60.0 mL of 10% NaOH was added to the suspension and stirred overnight. The pH was adjusted to approximately 3 using hydrochloric acid. The resulting brown precipitate was collected by centrifuge, washed with water, and dried under vacuum to yield **2** (8.0 g, 90%). $^1$H NMR (DMSO-$d_6$): $\delta$ 6.62 (s, 3H), 7.13 (d, 6H), 7.82 (d, 6H), 8.73 (s, 3H).

**Synthesis of PCN-100, $Zn_4O(TATAB)_2\cdot 17(DEF)\cdot 3(H_2O)$.** $H_3$TATAB (10.0 mg, 0.02 mmol) and $Zn(ClO_4)_2\cdot 6(H_2O)$ (30.0 mg, 0.08 mmol) were dissolved in DEF (1.5 mL) and sealed in a Pyrex tube under vacuum. The tube was held at 85 °C for three days to produce colorless block crystals. The crude product was washed with DEF to give pure PCN-100 (0.02 g, 0.007 mmol,

(30) Chae, H. K.; Siberio-Perez, D. Y.; Kim, J.; Go, Y.; Eddaoudi, M.; Matzger, A. J.; O'Keeffe, M.; Yaghi, O. M. *Nature* **2004**, *427*, 523–527.

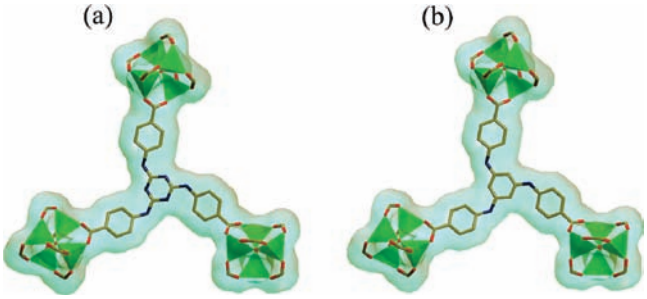


**Figure 1.** TATAB ligand of PCN-100 (a) and a BTATB ligand of PCN-101 (b) linked to three $Zn_4O(CO_2)_6$ SBUs.

70% yield based on TATAB) with a formula of $Zn_4O(TATAB)_2 \cdot 17(DEF) \cdot 3(H_2O)$. This formula was derived from crystallographic data, elemental analysis (calculated for $C_{133}H_{223}N_{29}O_{33}Zn_4$: C, 52.93; H, 7.45; N, 13.46. Found: C, 52.31; H, 7.47; N, 13.62%), and TGA.

**Synthesis of PCN-101, $Zn_4O(BTATB)_2 \cdot 16(DEF) \cdot 5(H_2O)$.** $H_3BTATB$ (3.0 mg, 0.006 mmol) and $Zn(NO_3)_2 \cdot 6(H_2O)$ (15.0 mg, 0.05 mmol) were dissolved in DEF (1.5 mL) and sealed in a Pyrex tube under vacuum. The tube was held at 85 °C for three days to produce colorless block crystals. The crude product was washed with DEF to give pure PCN-101 (0.006 g, 0.002 mmol, 67% yield based on BTATB) with a formula of $Zn_4O(BTATB)_2 \cdot 16(DEF) \cdot 5(H_2O)$. This formula was derived from crystallographic data, elemental analysis (calculated for $C_{134}N_{22}H_{222}O_{34}Zn_4$: C, 54.62; H, 7.59; N, 10.46. Found: C, 54.87; H, 7.68; N, 10.422%), and TGA.

**X-ray Crystallography.** Single-crystal X-ray data of PCNs-100 and -101 were collected on a Bruker Smart Apex diffractometer equipped with a low-temperature device and a fine-focus sealed-tube X-ray source (Mo Kα radiation, $\lambda$ = 0.71073 Å, graphite monochromated). The structure was solved by direct methods and refined by full-matrix least-squares on $F^2$ with anisotropic displacement using the *SHELXTL* software package.[31] Non-hydrogen atoms were refined with anisotropic displacement parameters during the final cycles. Hydrogen atoms on carbon were calculated in ideal positions with isotropic displacement parameters. In these structures, free solvent molecules were highly disordered, and attempts to locate and refine the solvent peaks were unsuccessful. The diffused electron densities resulting from these residual solvent molecules were removed from the data set using the *SQUEEZE* routine of *PLATON* and refined further using the data generated.[32] The contents of the solvent region are not represented in the unit cell contents in the crystal data. The details for data collection and refinement are included in the CIF file in the Supporting Information.

**Gas Sorption Measurements.** Gas sorption isotherm measurements were performed on an ASAP 2020 Surface Area and Pore Size Analyzer. Before the measurements, the samples of PCNs-100 and -101 were soaked in methanol for three days; during the exchange the methanol was refreshed nine times. The wet sample was then evacuated at ambient temperature for 24 h to remove the solvent molecules included and yield an activated sample. UHP-grade nitrogen (99.999%) gas source was used in the nitrogen sorption measurements. In the hydrogen sorption measurements, high purity hydrogen (99.9995%) was used. The temperature was maintained at 77 K with liquid nitrogen throughout each measurement.

**Capture of Metal Ions in PCN-100.** The reactions were performed in 5 mL of DMF (DMF = *N*,*N*-dimethylformamide) by adding 1 mmol of $Co(NO_3)_2$, $Cd(NO_3)_2$, or $HgCl_2$ to a sample of PCN-100 (about 100 mg) for 48 h at 60 °C. These samples were filtered, washed thoroughly with fresh DMF and methanol, and dried in air.

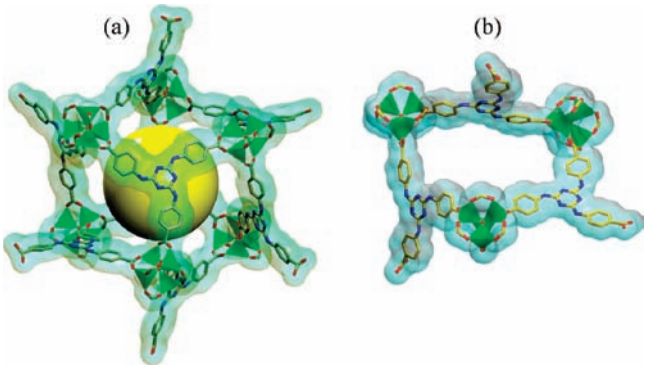


**Figure 2.** (a) Mesoporous cavity of PCN-100 with the internal diameter of 2.73 nm. (b) A window of (a) with about 1.32 nm ×1.83 nm.

**Knoevenagel Condensation Reaction Catalyzed by PCNs-100 and -101.** A solution of butyl cyanoacetate (0.21 mL, 1.5 mmol) and benzaldehyde (a, 0.15 mL, 1.5 mmol) (or 4-phenylbenzaldehyde (b, 0.27 g, 1.5 mmol) or benzophenone (c, 0.27 g, 1.5 mmol)) in dry DMSO-$d_6$ (10 mL) was mixed under a nitrogren atmosphere. The solution was transferred to a suspension of the PCN-100 and −101 (0.20 g, 0.06 mmol, 4 mol %) in DMSO-$d_6$ and was stirred at 50 °C for 2 h . The progress of the reaction was monitored by $^1$H NMR. The catalysts were removed by filtration, washed with DMSO and recovered.

## 3. Results and Discussion

**Structural Description.** X-ray single-crystal analysis revealed that PCNs-100 and -101 are isostructural (space group $Pa\bar{3}$); the following discussion of the crystal structure will focus on PCN-100. As expected, a regular $Zn_4O$ tetrahedron in PCN-100 was formed by a single O atom bonded to four Zn atoms, and then each edge of each Zn tetrahedron was capped by a $-COO^-$ group to build up a $Zn_4O(CO_2)_6$ cluster (Figure 1). The bond lengths of $Zn-O_{center}$ (1.7985(10)−1.9948(7) Å) are within the normal range, and the $Zn-O_{carboxylate}$ bond lengths (1.909(4)-2.015(3) Å) are close to those reported for other zinc-carboxylate donor compounds.[1] In this framework, six such $Zn_4O(CO_2)_6$ clusters as SBUs and eight TATAB ligands formed a mesoporous cavity with the internal diameter of approximately 2.73 nm (measured distance between opposite atoms); the size of the windows is about 1.32 nm ×1.82 nm (Figure 2). These mesoporous cavities are further interconnected through TATAB ligands to generate a 3-D noninterpenetrating extended open network, in which the vacant space is filled with seventeen guest DEF and three guest $H_2O$ molecules per formula unit (Figure 3). Removal of the guest molecules reveals that the effective free volume of PCN-100, calculated by PLATON analysis,[33] is 80.8% of the crystal volume (16462.7 Å$^3$ of the 20379.0 Å$^3$ unit cell volume). A clearer view can be obtained by reducing the framework of PCN-100 to a node-and-linker model, this is known as the topological approach.[34] Each $Zn_4O(CO_2)_6$ SBU and TATAB ligand can be defined as 6-connected and 3-connected node, respectively. Based on this simplification,

(31) Sheldrick, G. M. *Acta Crystallogr., Sect. A* **2008**, *64*, 112–122.
(32) Spek, A. L. *J. Appl. Crystallogr.* **2003**, *36*, 7–13.
(33) Vandersluis, P.; Spek, A. L. *Acta Crystallogr., Sect. A* **1990**, *46*, 194–201.
(34) O'Keeffe, M.; Eddaoudi, M.; Li, H. L.; Reineke, T.; Yaghi, O. M. *J. Solid State Chem.* **2000**, *152*, 3–20.

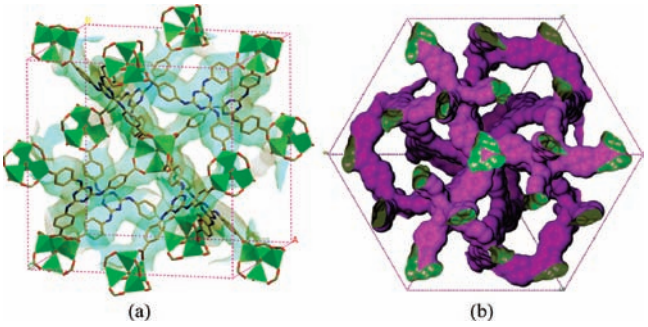


**Figure 3.** (a) View of packing of PCN-100. (b) A view of channels and free volume of PCN-100.

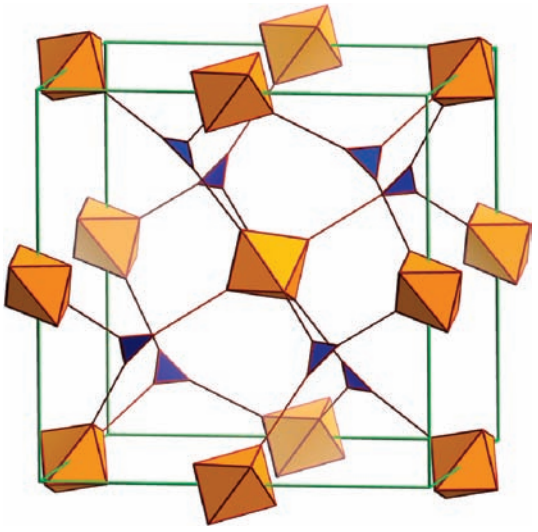

**Figure 4.** Topological structure (pyrite net) of PCN-100.

PCN-100 can be described as a 3,6-connected 3-D network with the Schläfli symbol $(6^{12}\cdot 8^3)(6^3)_2$, which corresponds to a pyrite (pyr) topology (Figure 4).[35]

**Thermogravimetric Analyses of PCNs-100 and -101.** The thermogravimetric analysis (TGA) curves of PCNs-100 and −101 are shown in Figures 5a and 5b, respectively. The TGA curve of PCN-100 showed a weight loss of 58.16% between 20 and 150 °C, which corresponds to the loss of 17 guest DEF and 3 guest $H_2O$ molecules (calculated 58.77%). Decomposition of PCN-100 began at about 300 °C. The residue was ZnO (experimental: 9.91% and calculated: 9.19%). Similar to that of PCN-100, the TGA curve of PCN-101 showed a weight loss of 57.82% between 20 and 150 °C, corresponding to the loss of 16 guest DEF and 5 guest $H_2O$ molecules (calculated 57.97%). Decomposition of PCN-101 also began near 300 °C. The residue was ZnO (experimental = 9.38% and calculated = 9.42%).

**Gas Sorption Properties.** The permanent porosity of mesoporous PCNs-100 and -101 is confirmed by their $N_2$ sorption isotherms at 77 K. Before the measurements, the samples of PCNs-100 and −101 were soaked in methanol and evacuated at ambient temperature for 24 h to obtain the activated samples. As shown in Figure 6, both of the $N_2$ sorption isotherms of PCNs-100 and −101 exhibit the

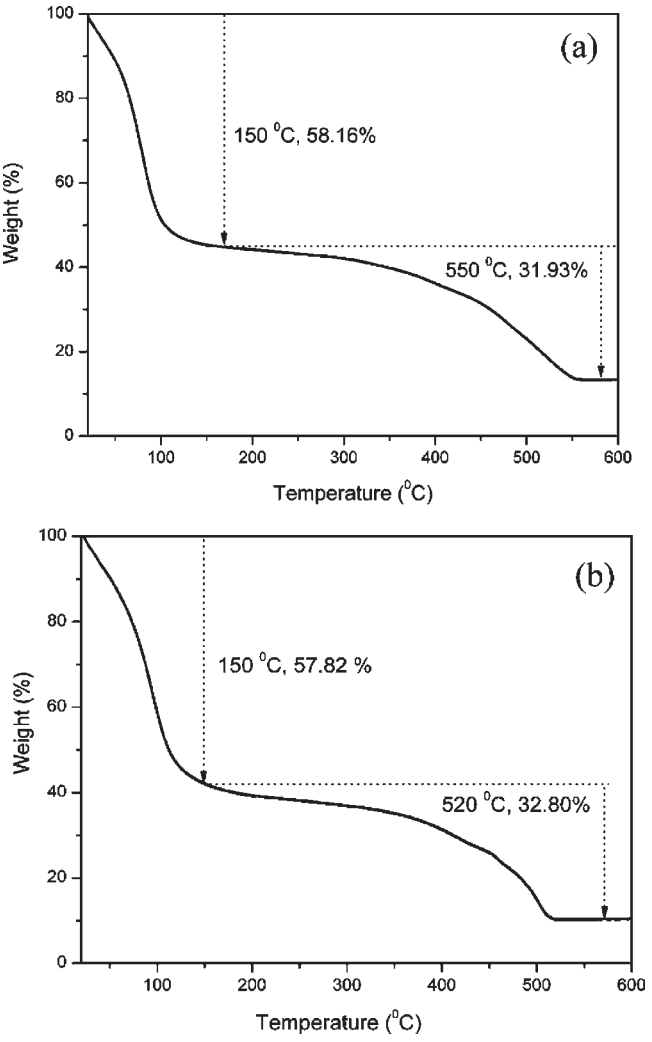


**Figure 5.** Thermogravimetric analyses (TGA) curves of PCN-100 (a) and -101 (b) under $N_2$ atmosphere.

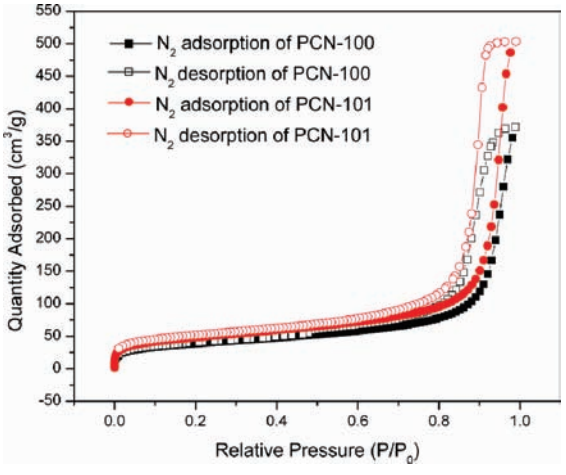


**Figure 6.** $N_2$ sorption isotherms with typical type IV behaviors of PCNs-100 and -101 at 77 K.

typical type IV behavior; that is, showing pore condensation with pronounced adsorption−desorption hysteresis (for additional support see pore size distribution in the SI). These results indicate the existence of mesopores

(35) Chae, H. K.; Kim, J.; Friedrichs, O. D.; O'Keefe, M.; Yaghi, O. M. *Angew. Chem., Int. Ed.* **2003**, *42*, 3907–3909.

**Scheme 2.** Possible Chelating Coordination Mode, Similar to That in Aminopyridinato Complexes, for Metal Ions in PCN-100

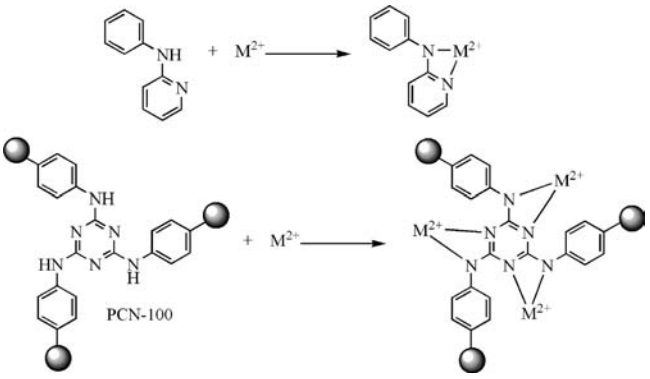


in PCN-100 and -101 with a maximum $N_2$ uptake of 371 $cm^3/g$ (Langmuir surface area of 860 $m^2/g$ and pore volume of 0.58 $cm^3/g$) and 503 $cm^3/g$ (Langmuir surface area of 1140 $m^2/g$ and pore volume of 0.75 $cm^3/g$), respectively. Low-pressure hydrogen sorption measurements were also performed at 77 K to investigate the $H_2$ uptake. The results showed that PCN-100 and -101 possess a maximum $H_2$ uptake of 0.35 wt % and 0.47 wt %, respectively (See Supporting Information).

**Capture of Different Metal Ions in PCN-100.** Encouraged by the possible chelating coordination mode, similar to that of aminopyridinato complexes, for metal ions in the TATAB ligand, we attempted to capture different metal ions within PCN-100. Capture of metal ions becomes particularly valuable when coordination of heavy metals such as cadmium and mercury is possible (Scheme 2). Aminopyridinato complexes of transition metals show a wide range of reactivities.[36,37] Since Cotton and co-workers[38] published an aminopyridinato complex, bis[2-(phenylamino)-pyridinato] bis(triphenylphosphino)ruthenium(II), in 1984, synthesis and characterization of this type of compounds has been a focus of a considerable amount of research in recent years.

The metal capture reaction was performed in a DMF solution of different metal salts ($Co(NO_3)_2$, $Cd(NO_3)_2$, or $HgCl_2$) and a sample of PCN-100. The products were characterized by XRD and ICP (See Supporting Information). A direct indication that a reaction between PCN-100 and Co(II) ions took place was the color of the solid changing from colorless to red (Figure S6). To verify Co(II) uptake, the $N_2$ adsorption isotherm, post metal addition, was compared to the result of the as-synthesized PCN-100 adsorption. The decreased adsorbed amount, presumably resulting from an increased density of the framework and the decreased pore sizes, indicates that Co(II) ions have been captured in the pores of PCN-100. Moreover, a concomitant change of the metal content of PCN-100 was observed by ICP corresponding to the impregnation of about 1.61 Co(II), 1.63 Cd(II), or 1.38 Hg(II) per formula, respectively. Similar experiments were performed on the isostructural PCN-101, which lacks the aminopyridinato-type chelating coordination environment.

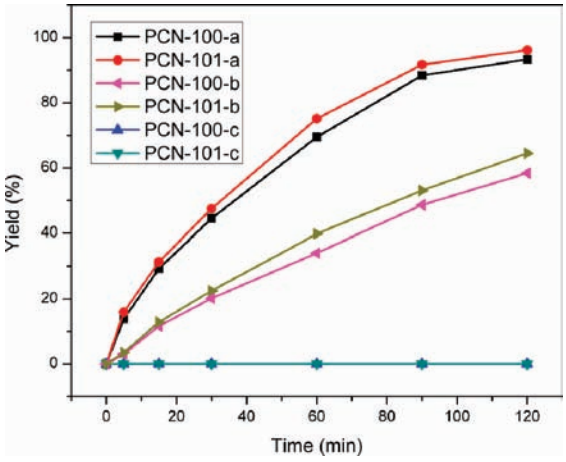


**Figure 7.** Conversion (%) vs time (min) for Knoevenagel condensation reaction of butyl cyanoacetate with benzaldehyde (a), 4-phenylbenzaldehyde (b) or benzophenone (c) in DMSO-*d*6 catalyzed by PCNs-100 and −101, respectively. Each conversion was detected by $^1H$ NMR based on starting material.

The ICP results showed that there was only 0.59 Co(II), 0.69 Cd(II), or 0.61 Hg(II) contained in the framework of PCN-101 per formula unit. From these results, it can be deduced that an additional 0.51 Co(II) ions were captured due to a chelating effect in PCN-100. Similarly, the ICP measurements revealed that there were an additional 0.47 Cd(II) or 0.39 Hg(II) ions captured due to this chelating effect. These interesting results suggest that PCN-100 and similar MOFs can be applied in the elimination of heavy metal ions from waste liquid.

**Knoevenagel Condensation Reaction Catalyzed by PCNs-100 and −101.** To explore the catalytic activity of mesoporous PCNs-100 and -101, Knoevenagel condensation reactions in the presence of these two MOFs were performed. The Knoevenagel reaction is a weakly basic, amine-catalyzed, condensation reaction that generates a C−C bond between an aldehyde or ketone and an methylene group containing active hydrogen atoms.[39−41] In order to test the size selectivity of the two MOFs, we took a systematic approach by varying the size and shape of the substrate. A solution of equivalent amounts of butyl cyanoacetate (0.58 nm ×0.10 nm) and benzaldehyde (a) (4-phenylbenzaldehyde (b) or benzophenone (c)) was mixed in DMSO-$d_6$. This solution was added at 323 K to suspensions of PCN-100 or −101 in DMSO-$d_6$ (Scheme 3) and the progress of the reaction was monitored by using $^1H$ NMR (See Supporting Information). As shown in Figure 7 and Table 1, benzaldehyde (size: 0.61 nm × 0.87 nm; shape: linear) leads to a 93% (96%) conversion catalyzed by PCN-100 (PCN-101). In the case of 4-phenylbenzaldehyde, a slightly elongated, linear molecule (0.61 nm × 1.33 nm), showed a 58% (65%) conversion. As for benzophenone, which is an angular molecule (0.66 nm × 1.14 nm), with the potential product extending in all three directions in an approximately trigonal plane fashion,

(36) Cotton, F. A.; Hillard, E. A.; Murillo, C. A.; Wang, X. P. *Inorg. Chem.* **2003**, *42*, 6063–6070.
(37) Cole, M. L.; Junk, P. C. *New J. Chem.* **2003**, *27*, 1032–1037.
(38) Chakravarty, A. R.; Cotton, F. A.; Shamshoum, E. S. *Inorg. Chim. Acta* **1984**, *86*, 5–11.
(39) Hasegawa, S.; Horike, S.; Matsuda, R.; Furukawa, S.; Mochizuki, K.; Kinoshita, Y.; Kitagawa, S. *J. Am. Chem. Soc.* **2007**, *129*, 2607–2614.
(40) Hwang, Y. K.; Hong, D. Y.; Chang, J. S.; Jhung, S. H.; Seo, Y. K.; Kim, J.; Vimont, A.; Daturi, M.; Serre, C.; Férey, G. *Angew. Chem., Int. Ed.* **2008**, *47*, 4144–4148.
(41) Gascon, J.; Aktay, U.; Hernandez-Alonso, M. D.; van Klink, G. P. M.; Kapteijn, F. *J. Catal.* **2009**, *261*, 75–87.

**Scheme 3.** Knoevenagel Condensation Reaction Catalyzed by PCNs-100 and -101

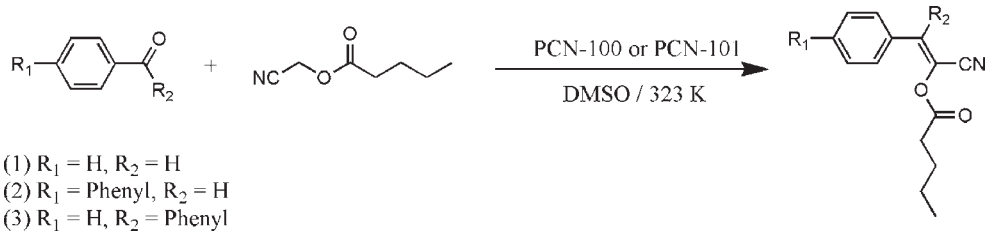


(1) $R_1$ = H, $R_2$ = H
(2) $R_1$ = Phenyl, $R_2$ = H
(3) $R_1$ = H, $R_2$ = Phenyl

**Table 1.** Knoevenagel Condensation Reaction of Butyl Cyanoacetate with Substrates Catalyzed by PCNs-100 and -101

| run | substrate | molecular size | catalyst | Conversion (%) |
|---|---|---|---|---|
| a |  | 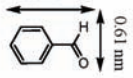  | PCN-100 | 93 |
| | | | PCN-101 | 96 |
| b | 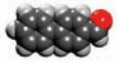 | 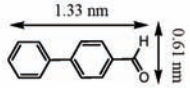  | PCN-100 | 58 |
| | | | PCN-101 | 65 |
| c | 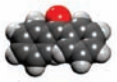 | 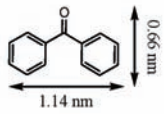  | PCN-100 | 0 |
| | | | PCN-101 | 0 |

reacted negligibly. The distinct conversion rates reflect size and shape selectivity of the two mesoporous catalysts. It is evident that these catalytic reactions happened within the mesopores of the two MOFs. If the reactions were catalyzed only on the external surface of the MOF crystals, we would see little difference in the conversion rates among the three substrates. An additional advantage of using PCNs-100 and −101 as catalysts is that they are easily isolated from the reaction suspension by a simple filtration and can be recycled with no observable loss of activity. The PXRD (powder X-ray diffraction) patterns of PCN-100 and −101 before and after the reactions were collected and examined; no loss of crystallinity was found, indicating high stability of the two mesoporous catalysts.

## 4. Conclusions

In summary, two isostructural mesoporous MOFs, PCNs-100 and -101, have been obtained by using $Zn_4O(CO_2)_6$ SBUs and two extended trigonal planar ligands containing amine functional groups. $N_2$ sorption isotherms of both PCNs-100 and -101 exhibit typical type IV behavior confirming their mesoporous nature. PCN-100 has been utilized to capture metal ions (Co (II), Cd(II), and Hg(II)), demonstrating application potential of mesoporous MOFs in the elimination of heavy metal ions from waste liquid. A second application of mesoporous MOFs tested was the selective catalysis of large molecules. A study has been conducted on the size and shape selectivity of PCNs-100 and -101 as catalysts in Knoevenagel condensation reactions. These results will facilitate the exploration of similar mesoporous MOFs for applications in selective catalysis as well as other fields such as heavy metal capture and drug delivery.

**Acknowledgment.** This work was supported by the U.S. Department of Energy (DE-FC36-07GO17033, hydrogen storage; DE-SC0001015, selective gas adsorption), the National Science Foundation (CHE-0930079), and the Welch Foundation (A-1706). We acknowledge Dr. Xi-Sen Wang for his help with the preparation of ligands.

**Supporting Information Available:** Crystallographic data (CIF), IR, PXRD, and $H_2$ adsorption data for PCNs-100 and -101, photos, PXRD, $N_2$ sorption isotherms, and ICP results for PCN-100 containing different metals, and NMR and PXRD spectra of PCNs-100 or −101 for catalytic reactions. These material are available free of charge via the Internet at http://pubs.acs.org.